Electronic Supplementary Information (ESI)

Nanotube Topography Rejuvenates the Senescence of Mesenchymal Stem Cells by Activating YAP Signalling

Yanping Sun,[a] Yejia Yu, [a] Shixing Ma, [a] Chengcheng Liao, [a] Jian Yang, [a] Yun Lyu, [a] Xuanhao Zhang, [a] Jingyi Zhang, [b] Weidong Tian [a] * and Li Liao [a] *

a. State Key Laboratory of Oral Diseases & National Clinical Research Center for Oral Diseases & Department of Pediatrics & Engineering Research Center of Oral Translational Medicine, Ministry of Education, West China Hospital of Stomatology, Sichuan University, 610041, Chengdu, China.

b. Chengdu Shiliankangjian Biotechnology Co.，Ltd.

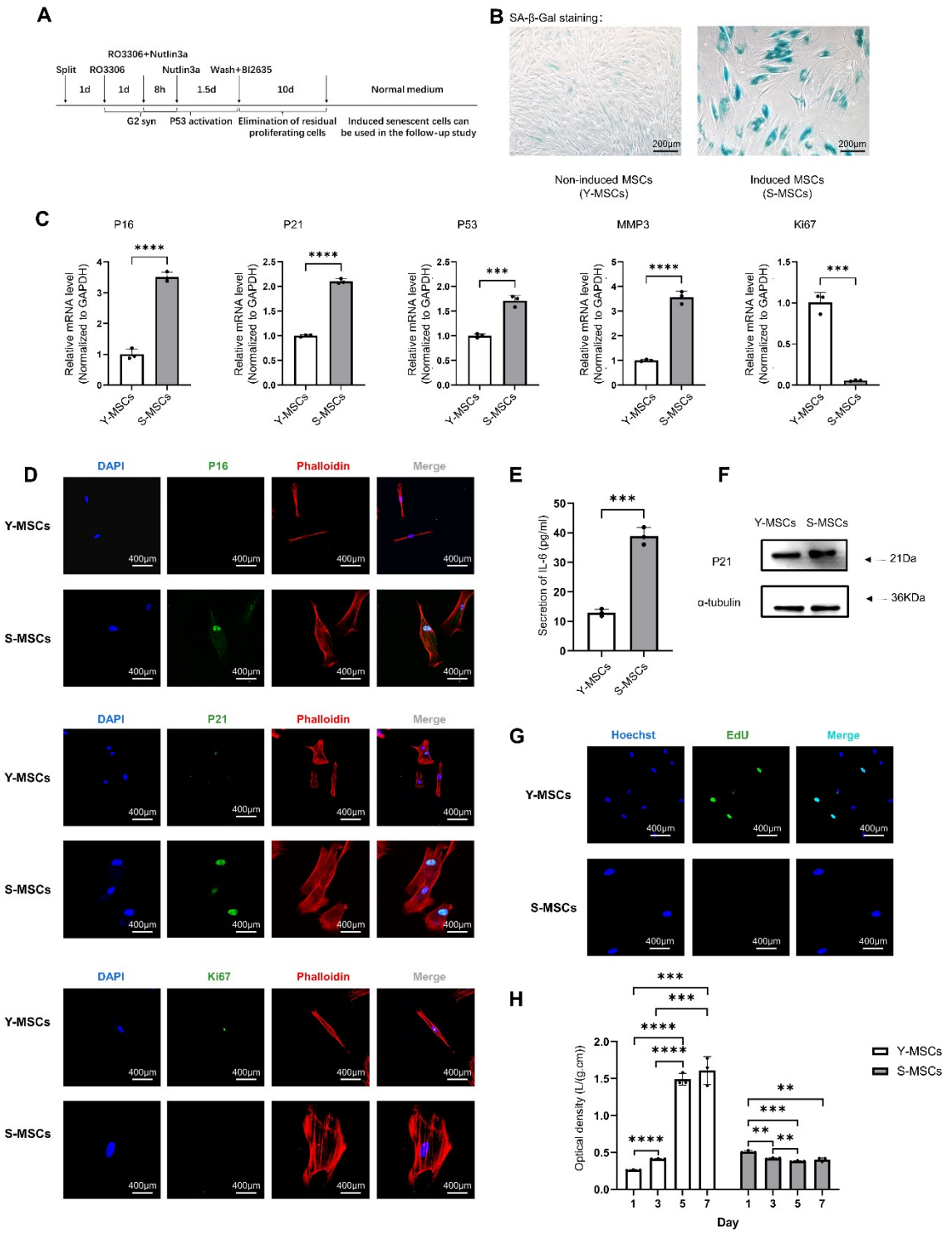

Figure S1. Induction and Characterization of Senescent Mesenchymal Stem Cells. (A) Schematic presentation illustrating the culture conditions for preparing S-MSCs. (B) SA-β-gal staining comparing Y-MSCs and S-MSCs. (C) qRT-PCR analysis of senescence-related genes (P16, P21, P53, MMP3, and Ki67) in Y-MSCs and S-MSCs. (D) Immunofluorescence staining of P16, P21, and Ki67 in Y-MSCs and S-MSCs. (E) ELISA analysis of IL-6 levels in Y-MSCs and S-MSCs cultures for 2 days. (F) Western blot analysis of p21 in Y-MSCs and S-MSCs. (G) EdU staining of Y-MSCs and S-MSCs. (H) Absorbance values of Y-MSCs and S-MSCs cultured for 1, 3, ,5, and 7 days detected using the CCK-8 assay. (*p < 0.05, **p < 0.01, ***p < 0.001, ****p < 0.0001)

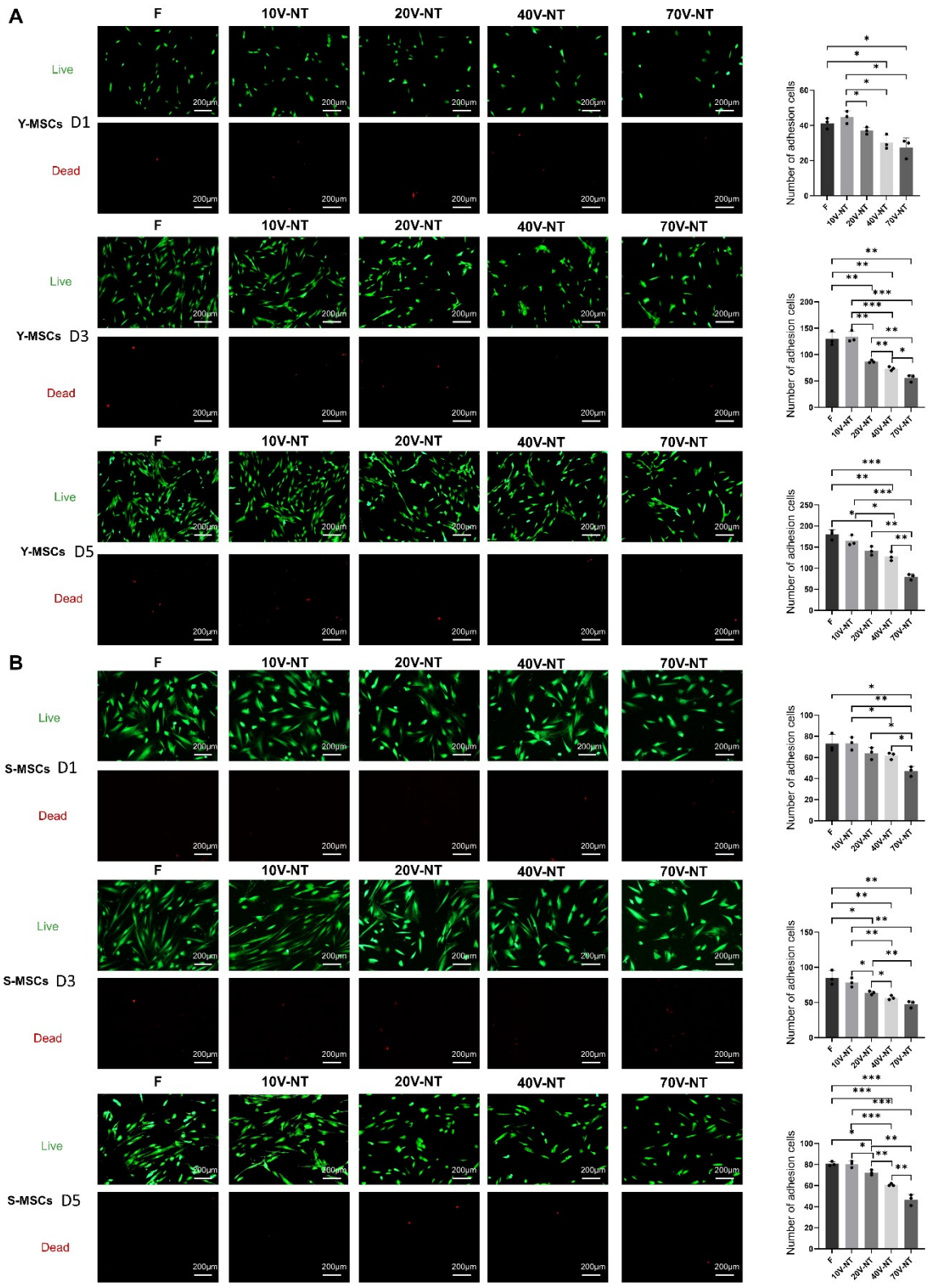

Figure S2. Cell viability and proliferation on nanotube topography. (A) Live/dead staining and quantification of Y-MSCs cultured on different nanotube topographies for 1,3, and 5days. (B) Live/dead staining and quantification of S-MSCs cultured on different nanotube topographies for 1,3, and 5days. (*p < 0.05, **p < 0.01, ***p < 0.001, ****p < 0.0001)

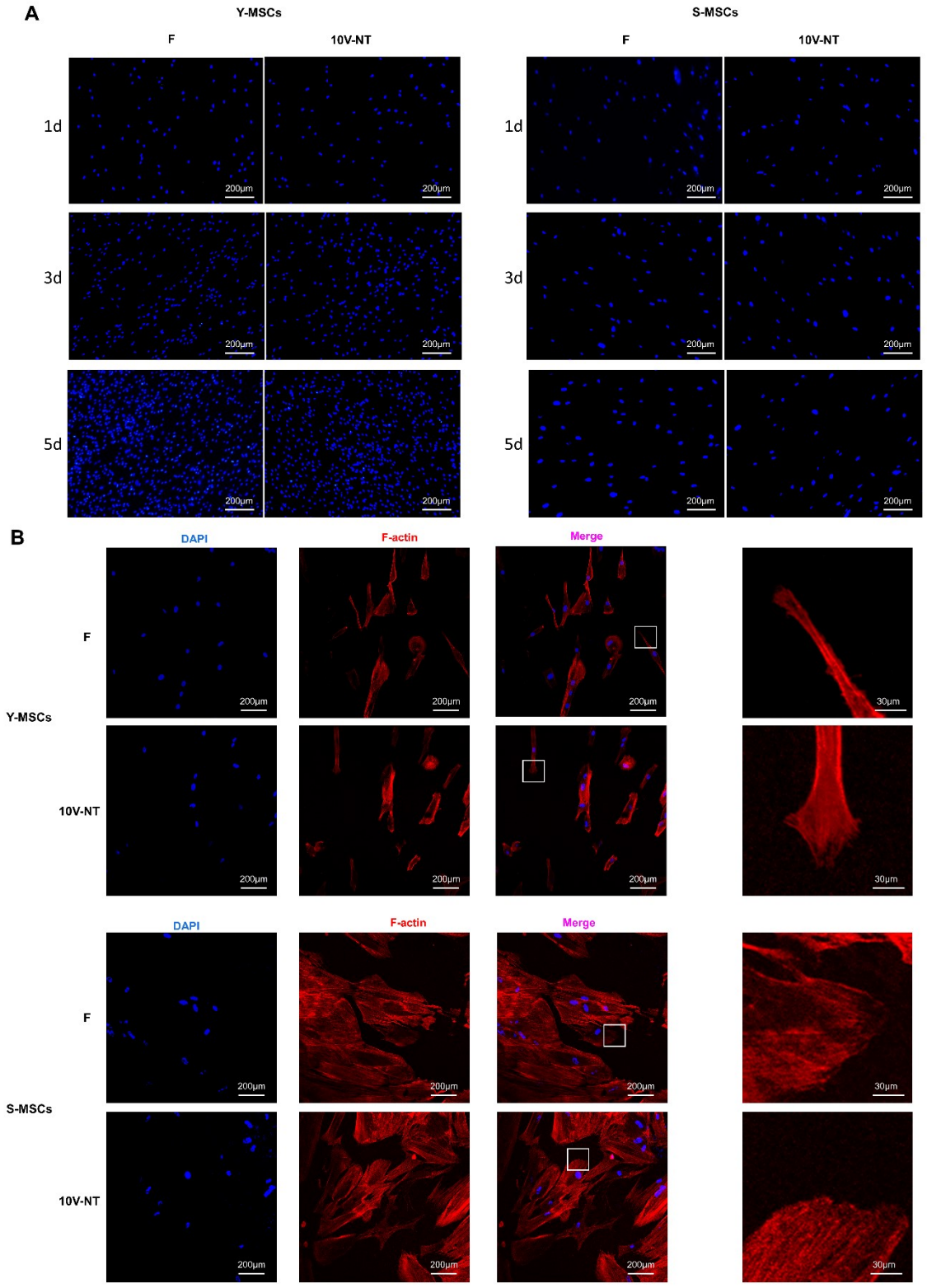

Figure S3. Cell growth and morphology on specialized nanotube topography. (A) Immunostaining of cells on specialized nanotube topography for 1, 3, and 5 days, assessed by DAPI. (B) Immunostaining of morphology of cells cultured on specialized nanotube topography for 2 days, assessed by F-actin immunostaining. The far right is the enlarged image inside the white box.

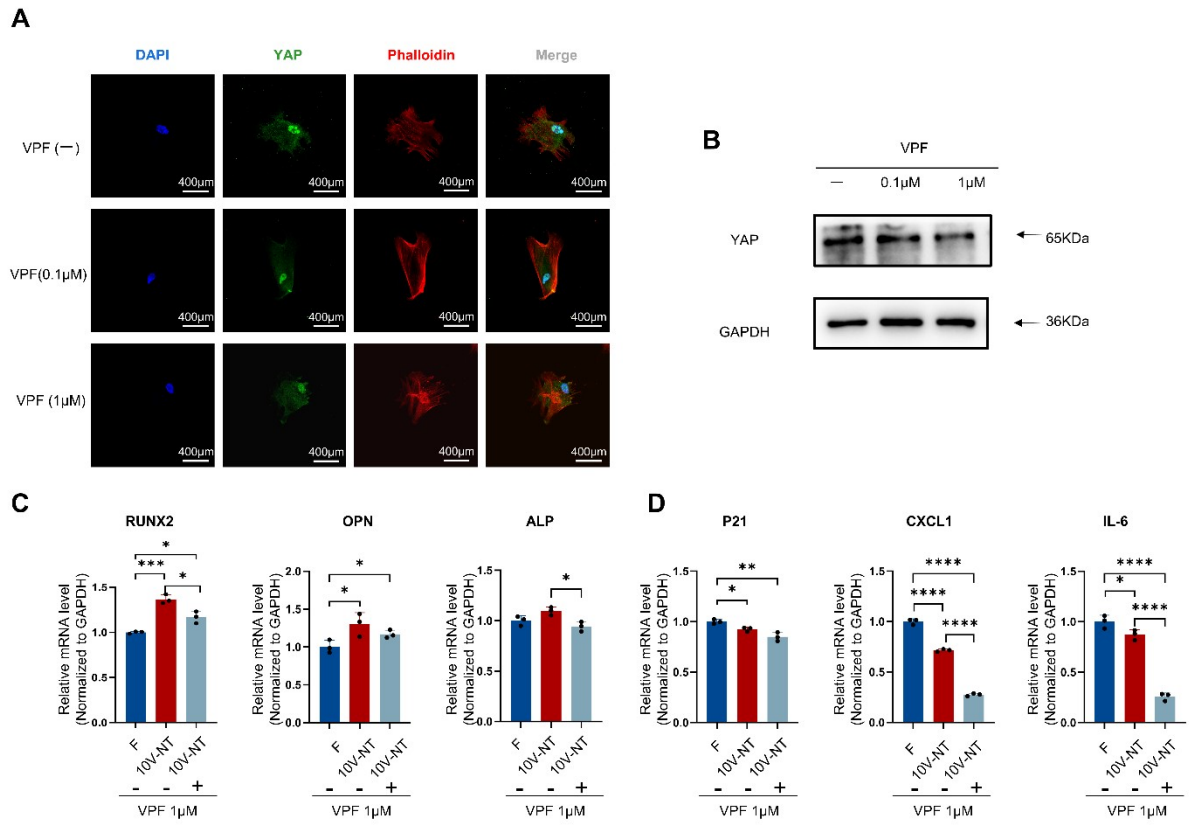

Figure S4. VPF impacts the influence of specialized nanotube topography on S-MSCs. (A) Immunofluorescence staining of YAP in S-MSCs treated with VPF(0.1μM and 1μM) for 2days. (B) Western blot analysis of YAP in S-MSCs treated with VPF (0.1μM and 1μM) for 2days. (C) qRT-PCR analysis of RUNX2, OPN, and ALP in S-MSCs cultured with osteogenic supplements and treated with VPF (1μM) on nanotube topography for 3 days. (D) qRT-PCR analysis of P21, CXCL1, and IL-6 in S-MSCs treated with VPF (1μM) cultured on nanotube topography for 2days. (*p < 0.05, **p < 0.01, ***p < 0.001, ****p < 0.0001)

Table S1 Antibodies used for WB and IF

Antibodies	Source	Identifier	Applications (dilution rate)
anti-Alkaline Phosphatase, Tissue non-specific antibody（2F4）	abcam	ab126820	WB (1:1000)
Lamin A/C (4C11)	Cell Signaling Technology	#4777	IF (1:100)
p16 INK4A (E6N8P) mAb	Cell Signaling Technology	#18769	IF (1:100)

Anti-p21 antibody [EPR3993]	abcam	ab109199	WB (1:1000); IF (1:100)
Anti-Ki67 antibody	abcam	ab15580	IF (1:100)
YAP(D8H1X)	Cell Signaling Technology	#14074	WB (1:1000); IF (1:100)
FAK rabbit pAb	Zen	343861	WB (1:1000)
p-FAK	Zen	381143	WB (1:1000)
GAPDH	Zen	200306-7E4	WB (1:2000)
anti-acetylated alpha tubulin antibody [6-11B-1]	abcam	ab24610	WB (1:1000)
Alexa Fluor 488 Goat anti Mouse	invitrogen	A11001	IF (1:200)
Alexa Fluor 488 Goat anti Rabbit	invitrogen	A11008	IF (1:200)
DAPI solution,1mg/ml	Solarbio	C0060	IF (1:1000)
Alexa Fluor 555 Phalloidin	Cell Signaling Technology	#8953	IF (1:200)
Goat Anti-Mouse IgG H&L（HRP）	Zen	511103	WB (1:2000)
Goat Anti-Rabbit IgG H&L（HRP）	Zen	511203	WB (1:2000)

Table S2 Primer sequences used for qRT-PCR analysis of gene expression

Gene	Forward primer	Reverse primer
P16	GCTTCCTGGACACGCTGGT	CATCTATGCGGGCATGGTTA
P21	GGGAGCAGGCTGAAGGGT	CGGCGTTTGGAGTGGTAGAA
P53	GCTTTGAGGTGCGTGTTTGTG	TTGGGCAGTGCTCGCTTAG
MMP3	TGAGGACACCAGCATGAACC	ACTTCGGGATGCCAGGAAAG
Ki67	TCCTTTGGTGGGCACCTAAGACCTG	TGATGGTTGAGGTCGTTCCTTGATG
BMP2	ACCCGCTGTCTTCTAGCGT	TTTCAGGCCGAACATGCTGAG

RUNX2	TGGTTACTGTCATGGCGGGTA	TCTCAGATCGTTGAACCTTGCTA
OPN	GAAGTTTCGCAGACCTGACAT	GTATGCACCATTCAACTCCTCG
OCN	CACTCCTCGCCCTATTGGC	CCCTCCTGCTTGGACACAAAG
ALP	ACTGGTACTCAGACAACGAGAT	ACGTCAATGTCCCTGATGTTATG
CXCL1	GCAGCAGGAGCGTCCGTGGC	CGGTTTGGGCGCAGTGGGGT
TNF-α	CCCAGGGACCTCTCTCTAATCA	GCTTGAGGGTTTGCTACAACATG
IL-6	TGTGAAAGCAGCAAAGAGGC	TGGGTCAGGGGTGGTTATT
MMP1	TGTTCTGGGGTGTGGTGTCT	CACACGCTTTTGGGGTTTGT
TGF-β	CTGTACATTGACTTCCGCAAG	TGTCCAGGCTCCAAATGTAG
ANKRD1	AGTAGAGGAACTGGTCACTGG	TGTTTCTCGCTTTTCCACTGTT
AXL	CCGTGGACCTACTCTGGCT	CCTTGGCGTTATGGGCTTC
GAPDH	CTTTGGTATCGTGGAAGGACTC	GTAGAGGCAGGGATGATGTTCT

Table S3 Compounds used in this study

Compounds	Source	Identifier	Concentration
RO3306	Selleck	S7747	9 μM
Nutlin3a	Selleck	S8059	5 μM
BI-2536	Selleck	S1109	100 nM
Verteporfin	Selleck	S1786	0.1 μM, 1 μM